Outline of a dielectric laser acceleration experiment at SwissFEL

E. Prat[a], S. Bettoni[a], M. Calvi[a], M. Dehler[a], F. Frei[a], P. Hommelhoff[b], M. Kozak[b], J. McNeur[b], C. Ozkan Loch[a], S. Reiche[a], A. Romann[a], R. Ischebeck[a]

[a] *Paul Scherrer Institut, CH-5232 Villigen PSI, Switzerland*
[b] *Department of Physics, Friedrich-Alexander-Universitt Erlangen Nrnberg (FAU), Staudtstr. 1, D-91058 Erlangen, Germany*

Abstract

The Accelerator on a Chip International Program (ACHIP), funded by the Gordon and Betty Moore Foundation for a 5 year period, pursues basic research and development for a super-compact accelerator on a chip, where the accelerating structure is a dielectric microstructure excited by femtosecond laser pulses. The Paul Scherrer Institute (PSI) will contribute to this by providing the international collaboration access to the high-brightness electron beams in SwissFEL, where we plan to do a proof-of-principle demonstration of the acceleration of a highly relativistic beam. In this contribution we present the conceptual layout of the experiment, in which we will focus the beam down to sub-micrometer beam sizes. Start-to-end simulation results of the tracked electron beam, and first calculations of the accelerating field of the microstructure will be shown.

1. Introduction

Dielectric laser acceleration (DLA), a modern technique based on a laser powering a dielectric microstructure, can achieve gradients in the GV/m range, implying a potential reduction of conventional accelerators' length by one order of magnitude or more [1]. The Accelerator on a Chip International Program (ACHIP) has the goal of carrying out research and development activities for DLA. The ACHIP program includes performing a proof-of-principle experiment of DLA at relativistic energies using the high-brightness beam delivered by SwissFEL [2] at the Paul Scherrer Institute (PSI). The goal is to demonstrate a gradient of 1 GV/m for a dielectric length of 1 mm, resulting in an acceleration of 1 MeV. In this document we present the current design of the DLA experiment that will be performed at SwissFEL from 2017, including the experiment location, the laser, the chamber and diagnostics. The main parameters of the experiment are shown in Table 1. We also present results of electron beam start-to-end simulations and acceleration calculations at the dielectric structure.

Table 1: Main parameters of the DLA experiment at SwissFEL.

Parameter	Value
Electron beam energy	3 GeV
Electron bunch charge	1 pC
Energy gain (goal)	1 MeV
Structure type	Double pillar
Accelerating length	1 mm
Accelerating gradient (goal)	1 GV/m
Structure diameter	1.2 μm (x) – 7.0 μm (y)
Laser wavelength	2 μm
Laser pulse energy	500 μJ
Laser pulse length (FWHM)	100 fs

DLA has already been demonstrated in several experiments —see for instance Refs. [1, 3, 4]. In all previous work, done at significantly lower energies than the ones that will be available at SwissFEL, the transverse dimensions of the beam were too large to travel through the structure without significant losses. Now at SwissFEL the goal is to accelerate all electrons that reach the structure. To achieve that, for the double-pillar structures of our experiment, the total transverse beam size should be smaller than 1.2 μm in the horizontal (x) and smaller than 7.0 μm in the vertical plane (y).

2. Experiment location

The DLA experiment will be carried out at SwissFEL, a free-electron laser (FEL) facility presently under construction at PSI that will serve two beamlines: Aramis, a hard X-ray beamline that will produce FEL radiation in 2017, and Athos, a soft X-ray beamline expected to lase by 2021. Figure 1 shows a schematic overview of the facility. The electrons are generated in an RF photoinjector. After that the beam is accelerated with S-band technology ($f \approx 3$ GHz) to an energy of 330 MeV and compressed in the first bunch compressor (BC1). The beam is then further accelerated with C-band RF structures ($f \approx 6$ GHz) and compressed to its final bunch length in the second bunch compressor (BC2). After Linac 2, a switchyard allows sending one bunch to the Athos beamline.

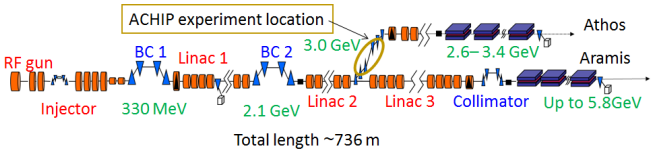

Figure 1: Schematic overview of the SwissFEL facility.

The rms beam size at a certain lattice position s is

$$\sigma(s) = \sqrt{(\epsilon_n/\gamma)\beta(s)}, \quad (1)$$

where ϵ_n is the normalized emittance, γ is the Lorentz factor of the electrons, and $\beta(s)$ is the β-function at the position s. To minimize the beam size at the structure, the measurement should be done at a location where the beam energy is the highest, i.e., after Linac 3 where the energy can be up to 5.8 GeV. Due to space constraints, however, the ACHIP experiment will be performed in the switchyard, where the energy is 3 GeV. This location will be available until the installation of a dechirper, with which the energy spread in the electron beam will be reduced from the year 2019. Afterwards it may be possible to continue the experiment behind the Athos undulators.

3. Electron beam

For the studies presented here, corresponding to the first experiments, the electron bunch length is longer than the laser wavelength. Consequently, the beam will not experience a net energy gain but an energy spread increase—an energy gain of 1 MeV corresponds to an rms energy spread increase of 0.71 MeV. To have a good resolution, the initial beam energy spread should be much smaller than the expected energy spread increase in the structure. In the near future we will investigate how to compress or bunch the beam such that all electrons are accelerated. Concerning the transverse beam size requirements, the normalized emittance has to be minimized at the photoinjector and the β-functions need to be very small at the structure (see Eq. 1). We use *ASTRA* [5] and *elegant* [6] to simulate the electron source and the rest of the accelerator, respectively.

3.1. Emittance and transport optimization

To minimize the emittance we use the procedure described in Ref. [7]. SwissFEL will operate with bunch charges between 10 and 200 pC. For the DLA experiment we will reduce the charge to 1 pC, a compromise between emittance (smaller for lower charges) and diagnostics resolution (better for higher charges). The gun laser of SwissFEL allows changing the rms pulse length between 300 fs and 10 ps or longer. We choose to have the shortest rms pulse length (300 fs) and smallest rms transverse beam size (50 µm), since even for these parameters the 1 pC beam is not affected by space-charge. For these conditions, the normalized projected emittance is 40 nm.

We have optimized the RF and compression setup after the injector to minimize the beam energy spread at the experiment location. We observe that without compression, the RF curvature in the S- and C-band stations would generate too large an energy spread of about 60 MeV. The final setup corresponds to a gentle compression of a factor ≈3 at BC1 by going 18 degrees off-crest in the last two injector structures, and no compression at BC2. Linac 1 is operated at an off-crest phase of 2.5 degrees to compensate the linear chirp required for the compression in BC1. The final rms bunch length is 92 fs and the rms energy spread is 42 keV, sufficiently small compared to the expected energy spread increase of about 1 MeV. The longitudinal phase space at the entrance of the experiment is shown in Fig. 2.

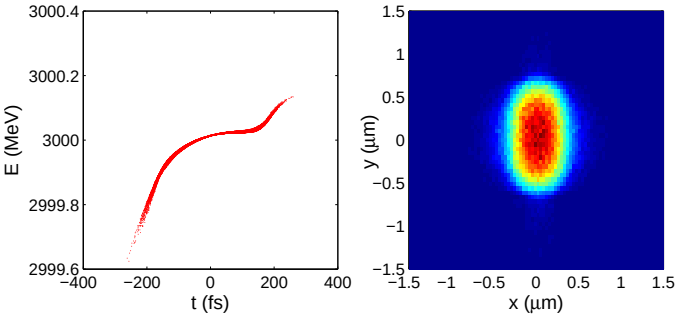

Figure 2: Longitudinal phase-space (left) and transverse profile (right) of the simulated electron beam at the experiment location. The rms pulse duration is 92 fs, the rms energy spread is 42 keV, and the rms beam sizes are 0.26 µm (horizontal) and 0.36 µm (vertical).

3.2. Beam optics

The design of the beam optics has two objectives: to focus the beam at the structure and to obtain an optimum resolution for the measurement, at a profile monitor, of the energy gain induced at the structure. The relative energy resolution at the profile monitor is $(\epsilon_n/\gamma)\beta_M/\eta_M^2$, where β_M and η_M are the β-function and dispersion values at the monitor location, respectively. The energy spread increase will be measured with a profile monitor installed in a dispersion section, where η is large by design—after the first dipole of an energy collimator in the switchyard and after the dump dipole in the Athos beamline.

Inside the experimental chamber, one triplet of permanent quadrupole magnets will be used to focus the electron beam at the structure, while a second identical triplet will rematch the beam back to the lattice. Permanent magnets are used since they can provide much higher fields than electromagnets. Each quadrupole has a magnetic length of 0.1 m and the distance between the quadrupoles of each triplet is 0.2 m. The structure will be placed in the center between the two triplets, 0.2 m after the last magnet of the first triplet. More details on the experimental chamber are given in Sec. 6.

The quadrupole settings are calculated using the optimizer of *elegant* [6]. With the exception of the two triplets, no additional quadrupoles will be needed to obtain the optics for the experiment: the electromagnetic quadrupoles installed for SwissFEL will be run at a different current than during nominal operation but their locations will remain the same. Figure 3 shows the optics along the lattice for the switchyard location. The β-functions at the structure are 1 cm and 1.8 cm in the horizontal and vertical directions, respectively, corresponding to rms beam sizes of 0.26 µm in the horizontal and 0.36 µm in the vertical plane (see Fig. 2), sufficiently small to guarantee the crossing of practically the full beam through the dielectric structure. At the profile monitor location, β_M is 2.9 m and η_M is 0.33 m. This corresponds to an energy resolution of 41 keV, small enough to detect the expected energy spread increase induced by the structure (≈1 MeV). Similar optics conditions can be obtained for the location after the Athos undulators. The first and the third quadrupole magnet of the triplet have a k value (geometric strength) equal to -25.89 m^{-2}, while the second magnet's k-value is 38.73 m^{-2}. We want the beam size at the structure to

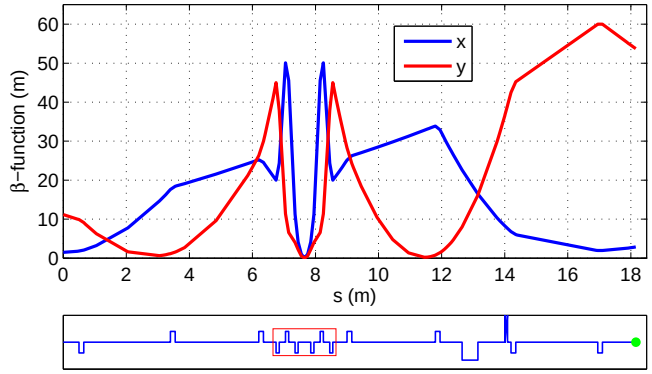

Figure 3: Horizontal (blue) and vertical (red) β-functions for the DLA experiment at the switchyard of SwissFEL. The lower sketch shows the corresponding magnetic lattice. The smaller rectangles mark the quadrupole magnets, the larger one shows the position of the dipole magnet before the profile monitor, indicated by a green circle. The red box defines the position of the experimental chamber with the two triplets and the accelerating structure in its center.

not increase more than 10% due to random field errors of the quadrupoles. To achieve that, our calculations show that the accuracy of the field stength of the permanent quadrupoles needs to be 0.2% or better.

4. Laser and timing

A commercial Ti:Sapphire oscillator with a regenerative amplifier (Coherent, Astrella) will likely be used as the laser source. The output from the amplifier system will be employed to pump an optical parametric amplifier (Light Conversion, TOPAS Prime) with a final output wavelength of 2 µm, a pulse energy of 500 µJ, a FWHM pulse length of 100 fs, and a repetition rate of 1 kHz. To match the longitudinal length of the dual-pillar structure, the spot size of the laser will be 1 mm in the direction of electron travel and 100 µm transversely, similar to matching aspect ratios obtained in previous experiments [4]. These laser parameters lead to an incident peak field strength of 4.9 GV/m. Given the planned 1 mm of interaction length between the electrons and the laser pulse and the 100 fs pulse length of the laser, pulse front tilting will need to be employed. Otherwise the moving electron pulse will be accelerated over a much shorter effective length, given by the laser pulse duration times the speed of light (i.e., 30 µm). This will involve introducing an angle of 45 degrees between the intensity and phase fronts of the laser via a dispersive reflective grating [8].

The synchronization of the laser will be based entirely on the SwissFEL synchronization scheme [9]. This requires the ACHIP laser oscillator to have the same specification (with respect to synchronization interfaces) as the laser systems employed in SwissFEL.

5. Structure

Figure 4 (left) shows the generic layout of the double-pillar structure that will be used for the experiment. It consists of a polycrystalline sapphire (Al_2O_3) substrate, on which there is a double row of pillars of the same material. The electron beam traverses the structure between these rows. The pillars, spaced at the free-space wavelength of 2 µm, longitudinally modulate the electric field, as necessary for net acceleration. Furthermore, we have a TE monopole type resonance inside the pillar, whose field enhancement can improve acceleration efficiency. This is also the reason for the interlaced positioning of the pillars. The total length of the structure is 1 mm, the pillar height is 7 µm, and the aperture for the electrons is 1.2 µm.

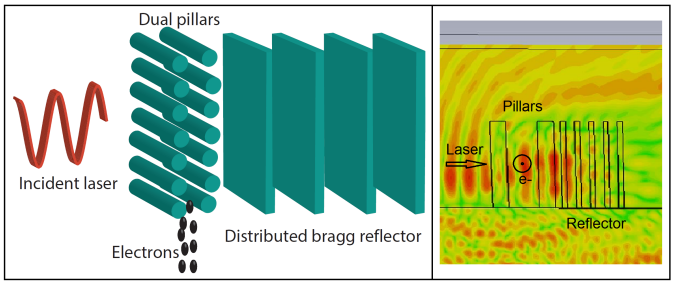

Figure 4: Left: Sketch of the dual-pillar structure with grating acting as a mirror. Right: Calculated longitudinal electric field distribution in transverse cut plane.

The ideal solution in terms of field symmetry would be to illuminate this double row of pillars symmetrically from both sides. But here, the light from both sides would need to be equal in amplitude and phase over the whole length of the structure (equivalent to 500 wavelengths), requiring very precise control of the transport of the laser beam. While this is doable with relatively minor efforts, we still opt for an approximate solution by using an asymmetric feed in combination with a grating acting as a symmetrizing mirror in the first experiments. Due to the substrate, the laser beam needs to be incident at a slight inclination of 5 degrees with respect to the horizontal plane.

We have done some preliminary calculations with this structure using *CST studio* [10]. Figure 4 (right) gives the transverse distribution of the longitudinal electric field, demonstrating the effectiveness of the grating in reflecting the incoming wave, and Table 2 shows the numerically computed acceleration for different positions in the structure aperture. These results are calculated for the steady-state and long-pulse condition. The structure dimensions were first optimized in 2D to realize the strongest longitudinal electric field in the center of the gap between the rows of pillars. However, the field symmetry between the pillars is not yet perfect, see Table 2. The peak in the gradient is horizontally offset and we observe a stronger variation in the complex phase. This not only leads to inhomogeneous acceleration, but also transverse deflection of the beam. The situation is more symmetric in the vertical plane, but here the amplitude variation is even more pronounced. A very encouraging result is the effect of the pillar resonance: we can obtain an effective accelerating gradient of roughly twice the amplitude of an incident plane wave, i.e., around 10 GV/m. Since our calculations are done for steady state and long pulse, however, we expect lower values, given our short laser pulse length. Nevertheless, the effective gradient in the structure will be limited by the breakdown limits of the structure material.

Further work will analyze the pillar resonance in more detail, and optimize the structure geometry based on more realistic simulations with a pulse-front-tilted beam to illuminate the full length of the structure. Following that, it is planned to use the calculated distribution of accelerating gradients and kicks in conjunction with the wakefields inside the structure to develop a model of the electrons' dynamics traversing the structure.

Table 2: Preliminary results calculated for the steady-state, long-pulse condition: mean accelerating gradient, normalized to incident laser free field amplitude versus position. The normalized beam position is centered between pillars and at 2.7 μm offset from the substrate.

position	$\lvert E_{acc}/E_0 \rvert$	$\arg(E_{acc})$ in deg.
center	1.87	40.6
x offset +0.5 μm	1.89	42.6
x offset −0.5 μm	2.00	36.2
y offset +0.5 μm	1.82	41.5
y offset −0.5 μm	1.80	41.9

6. Experimental chamber

The experimental chamber is displayed in Fig. 5. It consists of the dielectric microstructure, two triplets of permanent quadrupoles, an alignment stage for the structure, the laser coupling and relevant instrumentation in a two-meter vacuum chamber that can be placed on a girder. As shown in the figure, the vacuum chamber is laid out symmetrically around the interaction point. The chamber will be constructed during the summer and fall of 2016, and should be ready for installation in 2017.

The quadrupoles will have a volume of approximately $10 \times 10 \times 10\ \mathrm{cm}^3$ each, and an inner bore diameter of 2 mm. They can be aligned in both dimensions normal to the beam direction, and moved out of the beam horizontally. The transverse alignment and shift will be done with two translation stages angled by a few degrees. This allows for vertical movement of several millimeters, and horizontal movement of more than 10 cm, which is sufficient to remove the magnets completely from the beam axis, all without large forces on the actuators. Such a setup can be realized with in-vacuum translation stages.

The accelerating structure will be mounted on a hexapod that allows for alignment in all six degrees of freedom. A similar sample mount is in use at the Swiss Light Source at PSI, and we expect to profit from the design work and experience with this system. The goal for the vacuum is a pressure of 10^{-6} mbar.

7. Diagnostics

The diagnostics installed in the experimental chamber should allow verification of the electron beam optics as well as serve for the spatial and temporal alignment of the electron beam, the structure and the laser at the focus. Given the expected beam size, the spatial resolution should ideally reach 100 nm and cover an area of about 1 mm for both horizontal and vertical directions. The beam should be observable at different locations

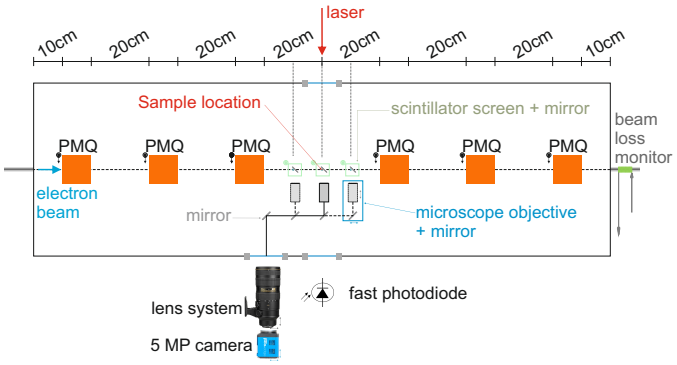

Figure 5: Setup of the different elements in the experimental chamber. PMQ stands for permanent magnet quadrupole.

in the vicinity of the focal plane. For this purpose, we plan to install three screens as indicated in Fig. 5, but only one movable imaging system that could be shared between the three screens. We will use a Ce:YAG screen, an in-vacuum, infinity-corrected microscope objective with a large working distance in combination with an out-of-vacuum lens and a 5-megapixel camera. To place and orient the DLA structure accurately, alignment holes of different sizes, machined in the support of the structure, could be used in combination with a beam-loss monitor located downstream of the chamber.

Concerning laser diagnostics, a noninvasive arrival-time monitor will register the laser pulses on an array of laterally spaced photodetectors after the electron bunch interaction zone and will compare it to the optical reference. The generated pulsed photocurrent will modulate the reference pulse train transmitted through an electro-optical intensity modulator, thus encoding the arrival time into the amplitude of the modulated pulse train, which can directly be sampled with a fast high-resolution analog-to-digital converter—similar to what is implemented for the SwissFEL bunch arrival-time monitor [11, 12] To read the tilt front we will compare the individual arrival times of the generated pulsed photocurrents of several photodetectors. To achieve high enough phase resolution the photocurrent (100 Hz repetition rate) will excite a high-Q RF cavity (GHz-range resonance frequency). The cavity leak-out signal will be down-converted to an intermediate frequency using a mixer and thus preserving the phase resolution. Phase information will be retrieved from reading the DC voltages of our extremely stable and well characterized RF phase detector.

The temporal overlap between laser and electron beam has to be set and verified. For that we propose using a transition radiator in the focal plane. A thin titanium foil, placed under an angle of 45 degrees with respect to the electron beam axis, will generate coherent transition radiation in a broad spectral range in a direction colinear with the partially transmitted laser. By using an arrangement of fast photodiodes, probably for two different wavelenghts for separate detection of the driving laser pulses and the transition radiation, timing overlap between the electrons and the laser could be determined by benefiting from the readout architecture of the previously described laser arrival-time monitor before inserting the structure in the focal plane.

8. Conclusion and outlook

We have presented the initial design of the DLA experiment to be performed at SwissFEL from 2017 within the ACHIP collaboration. All key components such as the laser, the dielectric structure, and the chamber with its diagnostics have been specified and will be available for the experiments. Our simulation results show that the electron beam will traverse the structure without losses, and first calculations indicate that we should be able to demonstrate an acceleration gradient in excess of 1 GeV/m. Next steps include the optimization of the structure geometry based on more realistic field calculations, simulations of higher compression or bunching of the electrons, delivery of the laser and other components, production of the structures, and damage tests at the SwissFEL injector.

9. Acknowledgments

Many thanks go to Thomas Schietinger for a careful proofreading of the manuscript. This work is supported by the Gordon and Betty Moore Foundation.

[1] R. J. England *et al.*, Rev. Mod. Phys. **86**, 1337 (2014).
[2] R. Ganter (ed.), PSI Report No. 10-04, 2012.
[3] J. Breuer and P. Hommelhoff, Phys. Rev. Lett. **111**, 134803 (2013).
[4] E. A. Peralta *et al.*, Nature **503**, 91 (2013).
[5] K. Floettmann, ASTRA User's Manual, 2000, `http://www.desy.de/~mpyflo/Astra_dokumentation/`.
[6] M. Borland, APS LS Note No. 287, 2000.
[7] S. Bettoni, M. Pedrozzi, and S. Reiche, Phys. Rev. ST Accel. Beams **18**, 123403 (2015).
[8] T. Plettner and R. L. Byer, Phys. Rev. ST Accel. Beams **11**, 030704 (2008).
[9] S. Hunziker, V. Arsov, F. Buechi, M. Kaiser, A. Romann, and V. Schlott, in *Proceedings of the 3rd International Beam Instrumentation Conference, Monterey, CA, USA, 2014* (Jacow, Geneva, 2015), p. 29.
[10] CST Microwave Studio, Computer simulation technology. GmbH, Darmstadt, Germany (2009).
[11] V. Arsov, M. Dehler, S. Hunziker, M. Kaiser, and V. Schlott, in *Proceedings of the 2nd International Beam Instrumentation Conference, Oxford, UK, 2013* (Jacow, Geneva, 2013), p. 8.
[12] V. Arsov, M. Aiba, M. Dehler, F. Frei, S. Hunziker, M. Kaiser, A. Romann, and V. Schlott, in *Proceedings of the 36th International Free Electron Laser Conference, Basel, Switzerland, 2014* (Jacow, Geneva, 2015), p. 933.